

Introduction

Two-dimensional transition-metal dichalcogenides are a class of layered semiconducting materials that exhibit unique layer-number-dependent optical and electronic properties. In this application note, the transition-metal dichalcogenide tungsten diselenide (WSe₂) is characterised using the RMS1000 Confocal Microscope with five imaging modalities: reflected brightfield & darkfield, Raman, photoluminescence and second harmonic generation to fully characterise its layer-dependent optoelectronic properties.

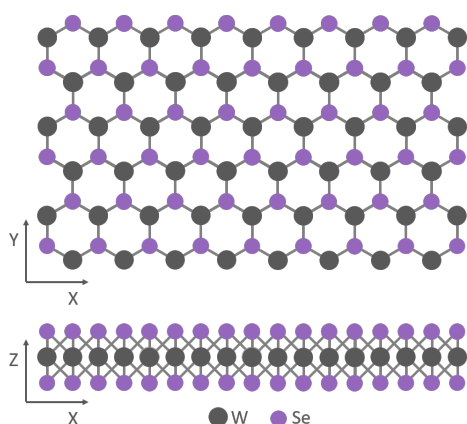


Figure 1: Monolayer WSe₂ Crystal Structure.

Materials & Methods

WSe₂ crystals were grown on a Si substrate using chemical vapour deposition (CVD) and characterised using an Edinburgh Instruments RMS1000 Confocal Microscope. The RMS1000 was equipped with a 100x NA 0.9 objective and a back-illuminated CCD camera. For Raman and photoluminescence imaging, the WSe₂ was excited with a 532 nm laser using a

1800 gr/mm and 300 gr/mm diffraction grating to acquire the Raman and photoluminescence spectra respectively. For second harmonic generation (SHG) imaging, a Chromacity 1040 HP femtosecond fibre laser (Chromacity Ltd. UK) operating at 1040 nm and 80 MHz was coupled to the RMS1000 for excitation, and the SHG response was acquired using a 300 gr/mm diffraction grating.



Figure 2: Edinburgh Instruments RMS1000 Multimodal Confocal Microscope.

Brightfield and Darkfield Imaging

The WSe₂ crystal was first widefield imaged using reflected brightfield and darkfield (Figure 3). In brightfield, the reflective silicon substrate appears bright and the absorbing WSe₂ crystal deposited atop is darker. Nucleation sites appear as dark spots across the crystal surface, as well as a stronger absorbing domain in the centre that is suggestive of multilayer WSe₂.

In darkfield, the sample is illuminated at an oblique angle and steps in sample surface height cause increased scattering and appear bright in the image. The darkfield image reveals there are two regions in the central domain with different heights, likely due to different WSe₂ layer numbers.

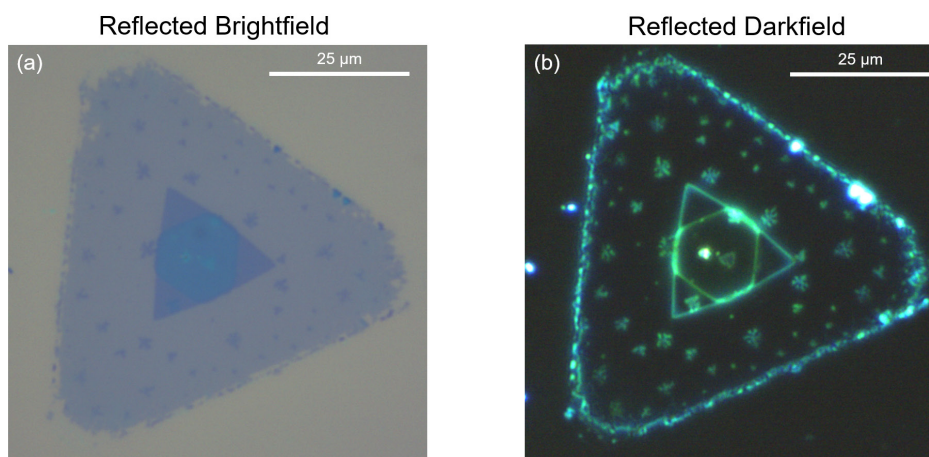


Figure 3: (a) Reflected brightfield and (b) reflected darkfield imaging of the WSe₂ crystal.

Raman Imaging

The crystal was next Raman imaged (Figure 4). WSe₂ has a characteristic Raman peak at 250 cm⁻¹ (Figure 4d) which corresponds to the in-plane E_{2g}¹ and out-of-plane A_{1g} phonon modes of WSe₂. In contrast to other transition-metal dichalcogenides, the E_{2g}¹ & A_{1g} phonon modes are almost degenerate in WSe₂ and are not individually resolved, with both contributing to the 250 cm⁻¹ peak.^{1,2} In the centre of the crystal, an additional peak at 310 cm⁻¹ is observed (marked with arrows in Figure 4d). This peak is symmetry forbidden in monolayer WSe₂ and indicative of multilayer WSe₂.²

The E_{2g}¹/A_{1g} peak intensity (Figure 4a) is highest in the large primary triangle domain, and reduces by ~80% within the inner triangle domain. The reduction in E_{2g}¹/A_{1g} intensity is indicative of a change from monolayer to multilayer WSe₂.¹ The E_{2g}¹/A_{1g} peak position (Figure 4b) shifts from 250 cm⁻¹ in the primary

domain to 247 cm⁻¹ within the inner domain which supports a change in layer number.³ The E_{2g}¹/A_{1g} peak also shifts towards higher wavenumbers at the edges of the crystal which is attributed to changes in the local microenvironment at the disordered edges.

Ramacle[®] spectral matching analysis (Figure 4c) identified three distinct Raman spectral regions in the crystal. In spectral matching, spectra at user-selected locations in the map are designated as archetypes and the deviation of all other spectra in the map from the archetype is calculated. Lower deviations from the archetype spectra are represented by more intense colour. The monolayer WSe₂ primary domain is highlighted in blue while the inner domain was found to be composed of two regions (highlighted in red and green) with subtly different E_{2g}¹/A_{1g} peak shapes. This agrees with the change in surface height in the inner domain observed in the darkfield image.

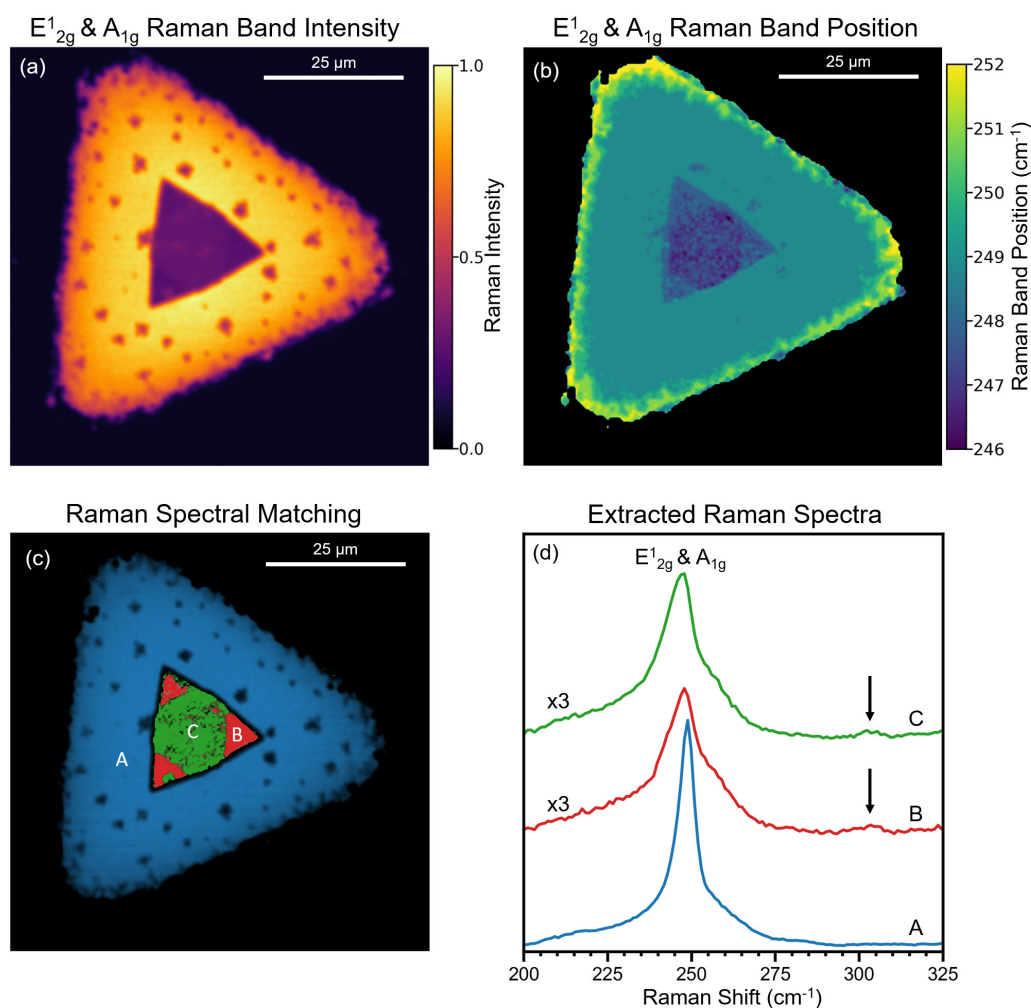


Figure 4: Raman imaging of WSe₂. (a) Intensity of the E_{2g}¹/A_{1g} (250 cm⁻¹) Raman band, (b) peak position of the E_{2g}¹/A_{1g} Raman band, (c) least squares spectral matching revealing three distinct Raman spectral areas, (d) averaged Raman spectra from areas A, B and C; spectra B and C are scaled in intensity by a factor of three and the arrows mark the location of the multilayer 310 cm⁻¹ peak. The Raman imaging parameters were: 40 x 40 μm², 200 x 200 pixels, 50 ms integration time, 532 nm laser, 1800 gr/mm diffraction grating, 300 μm pinhole.

Photoluminescence Imaging

To obtain additional insight into the inner domain, the crystal was photoluminescence (PL) imaged (Figure 5). The total PL intensity (Figure 5a) is lower within the inner domain, and the PL peak position (Figure 5b) red-shifted. Spectral matching (Figure 5c) identified four distinct PL spectral regions across the crystal and their corresponding spectra are shown in Figure 5d.

Region A (blue) is monolayer WSe₂ with PL peak at 780 nm from confined exciton emission. In region B the total PL intensity is decreased with a longer wavelength shoulder peak at 870 nm, while in region C the PL intensity decreases further and spectral weight shifts to the long wavelength shoulder. It has been established that as the number of layers increases in WSe₂, the PL emission red-shifts from exciton based emission at ~1.6 eV (~780 nm) in the monolayer to indirect bandgap emission at

~1.2 eV (~1000 nm) in bulk WSe₂.¹ Region B and C are therefore assigned as bilayer and trilayer WSe₂ respectively. Similarly to the Raman image, significant edge effects were also observed in the PL, with the PL peak position blue-shifted on the lower edge (spectrum D) and red-shifted on the upper edge of the crystal.

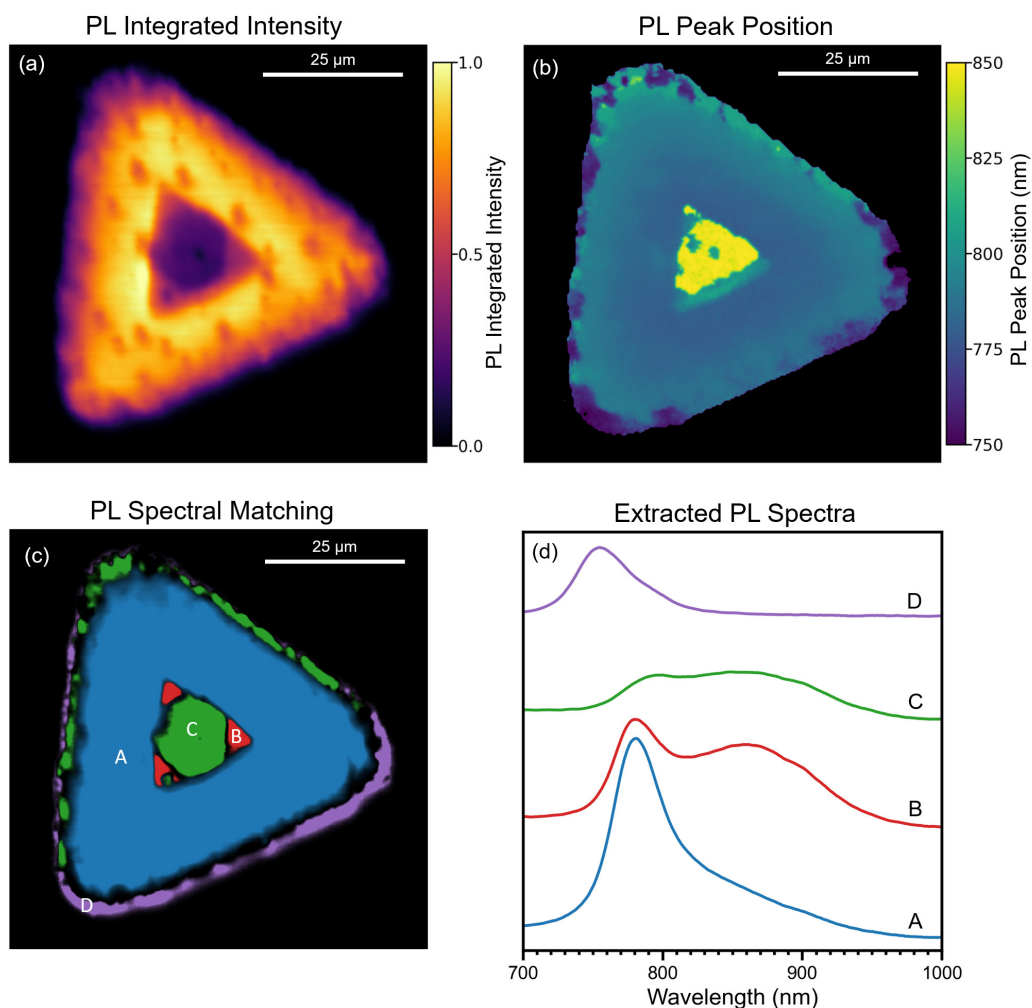


Figure 5: Photoluminescence imaging of WSe₂. (a) Integrated intensity of the PL response, (b) PL primary peak position, (c) least squares spectral matching revealing four distinct PL spectral areas, (d) averaged PL spectra from areas A, B, C and D. The PL imaging parameters were: 40 x 40 μm², 200 x 200 pixels, 30 ms integration time, 532 nm laser, 300 gr/mm diffraction grating, 300 μm pinhole.

Second Harmonic Generation Imaging

To determine the layer orientation within the three identified domains, the crystal was imaged using second harmonic generation (SHG) (Figure 6). SHG imaging is highly sensitive to the crystalline symmetry of transition metal dichalcogenides, with SHG only occurring when there is a non-centrosymmetry in the excitation focal volume. Monolayer WSe₂ is non-centrosymmetric and region A has a measurable SHG response as expected. The symmetry of multilayer WSe₂ depends on the type of layer stacking, 2H or 3R.⁵ In 3R stacking, each layer has the same orientation and the multilayer is non-centrosymmetric with SHG response increasing with layer number. In contrast, in 2H stacking, each layer is rotated 180° with respect to the adjacent layers and odd-numbered multilayers are net non-centrosymmetric with an SHG response similar to the monolayer while even-numbered multilayers are net centrosymmetric with no SHG response.^{4,5}

The bilayer WSe₂ in region B has an SHG response that is twice that of the monolayer, and the two layers therefore must be 3R stacked. The trilayer WSe₂ in region C has diminished SHG response compared to the monolayer which indicates the third layer in the trilayer is rotated relative to the first and second layers resulting in a partial restoration of centrosymmetry. The blue, red and green dashed triangles in Figure 6a illustrate the relative orientations of the three layers in the crystal. The growth of the third layer (green) has terminated at the boundaries of the second layer (red) resulting in a partial triangle.

Conclusion

Through a combination of widefield, Raman, PL and SHG imaging techniques, the layer number and stacking type in a CVD-grown WSe₂ crystal was identified. The multimodal capabilities of the RMS1000 Confocal Microscope make it an ideal imaging platform for studying the optoelectronic properties of transition-metal dichalcogenides.

References

1. Todddorf *et al.*, Photoluminescence emission and Raman response of monolayer MoS₂, MoSe₂, and WSe₂, *Opt. Express*, 2013, **21**, 4908-4916
2. Ribeiro-Soares *et al.*, Second Harmonic Generation in WSe₂, *2D Mater.*, 2015, **2**, 045015
3. Terrones *et al.*, New First Order Raman-active Modes in Few Layered Transition Metal Dichalcogenides, *Sci. Rep.*, 2014, **4**, 4215
4. Zhao *et al.*, Atomically phase-matched second-harmonic generation in a 2D crystal, *Light Sci. Appl.*, 2016, **5**, e16131
5. Shinde *et al.* Stacking-controllable interlayer coupling and symmetric configuration of multilayered MoS₂, *NPG Asia Mater.*, 2018, **10**, e468



For more information, please contact:
+44 (0) 1506 425 300
sales@edinst.com

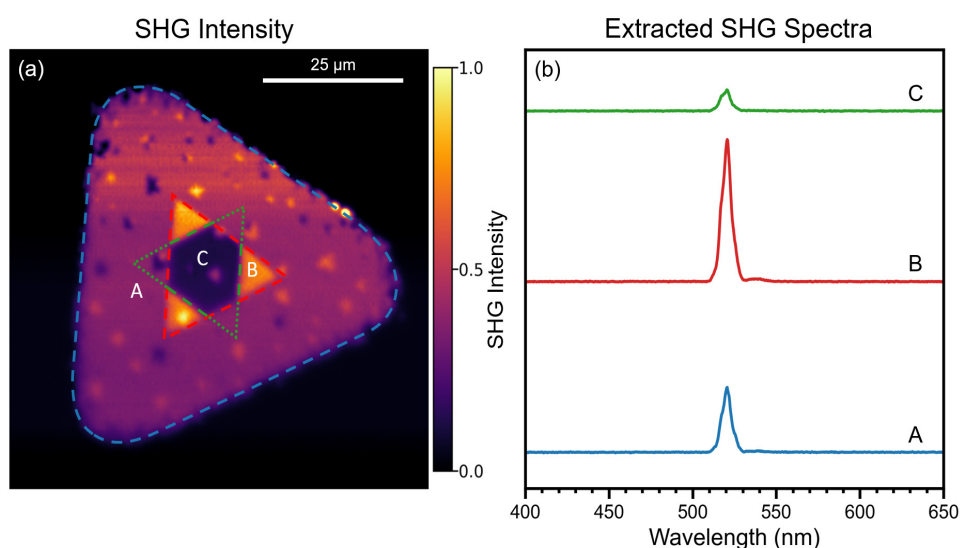


Figure 6: Second Harmonic Generation imaging of WSe₂. (a) Intensity of the SHG peak at 520 nm. (b) extracted SHG response from areas A, B, and C. The SHG imaging parameters were: 40 x 40 μm², 200 x 200 pixels, 11 ms integration time, 1040 nm femtosecond pulsed laser, 300 gr/mm diffraction grating, 300 μm pinhole.